DOI: 10.1002/ejic.201000121

$AlMe_3$, $GaMe_3$ and $InMe_3$ Adducts of *N*,*N*-Bis(2-{pyrid-2-yl}ethyl)-hydroxylaminato Rare-Earth Metal Complexes and Their Molecular Dynamics

Benjamin J. Hellmann,[a] Andreas Mix,[a] Beate Neumann,[a] Hans-Georg Stammler,[a] and Norbert W. Mitzel*[a]

In memoriam Professor Dr. Herbert Schumann

Keywords: Rare earths / Hydroxylamines / Hemilability / N,O-Ligands / Molecular dynamics

Reactions of hydroxylaminato rare-earth metal complexes of the general type $[Cp_2Ln\{\eta^2\text{-}ON(C_2H_4\text{-}o\text{-}Py)_2\}]$ (Cp = cyclopentadienyl, Py = pyridyl, Ln = Y, Sm, Nd, Pr, La) with the Lewis acids $AlMe_3$, $GaMe_3$ and $InMe_3$ resulted in the formation of the oxygen bonded adducts $[Cp_2Ln\{\eta^2\text{-}ON(C_2H_4\text{-}\eta^1\text{-}o\text{-}Py)(C_2H_4\text{-}o\text{-}Py)\}\cdot EMe_3]$ where Ln = Y, Sm and E = Al, Ga, In. Combination of the corresponding Nd, Pr and La complexes with the Lewis acids EMe_3 gave the doubly pyridyl coordinated complexes $[Cp_2Ln\{\eta^2\text{-}ON(C_2H_4\text{-}\eta^1\text{-}o\text{-}Py)_2\}\cdot EMe_3]$ (E = Al, Ga, In). Reactions of the complexes $[Cp_2Ln\{\eta^2\text{-}ON(C_2H_4\text{-}o\text{-}Py)_2\}]$ with two equivalents of the Lewis acids reveal complexes of the type $[Cp_2Ln\{\eta^2\text{-}ON(C_2H_4\text{-}\eta^1\text{-}o\text{-}Py)(C_2H_4\text{-}o\text{-}Py)\}\cdot 2EMe_3]$ (Ln = Y, Sm and E = Al, Ga, In) in which one Lewis acid EMe_3 coordinates to the hydroxylaminato oxygen atom and one interacts with a pyridyl nitrogen atom. The possibility of synthesising heterotrimetallic complexes was demonstrated by reacting the compound $[Cp_2Y\{\eta^2\text{-}ON(C_2H_4\text{-}\eta^1\text{-}o\text{-}Py)(C_2H_4\text{-}o\text{-}Py)\}\cdot AlMe_3]$ with $GaMe_3$ to obtain the complex $[Cp_2Y\{\eta^2\text{-}ON(C_2H_4\text{-}\eta^1\text{-}o\text{-}Py)(C_2H_4\text{-}o\text{-}Py)\}\cdot AlMe_3\cdot GaMe_3]$. The compounds have been characterised by elemental analysis, NMR spectroscopy (except paramagnetic substances) and single-crystal X-ray diffraction experiments. The aggregation trend is found to be directly related to the size of the metal ions. The new complexes exhibit a highly dynamic behaviour in solution. The two pyridyl nitrogen atoms are changing their coordination to the metal atom rapidly at ambient temperature even when the pyridine nitrogen donor atom is blocked by an EMe_3 unit. VT-NMR experiments showed that this dynamic exchange can be frozen on the NMR time scale.

Introduction

The large variety of hydroxylaminato compounds of the metal ions of group 4,[1] 12,[2] 13[3] shows the high flexibility of $[R_2NO^-]$ ligands in coordination chemistry. These ligands can complex metal atoms e.g. by end-on coordination, side-on coordination, μ-O-end-on coordination or μ-O-side-on coordination mode to exemplify only four of the explored binding motifs.

The special binding characteristics of hydroxylamines to act as side-on coordinating ligands has even been demonstrated for the main-group elements silicon and germanium, where they lead to the formerly unexpected formation of SiON[4] and GeON[5] three-membered ring systems. Hydroxylaminato ligands also offer the possibility to form multinuclear aggregates by bridging several metal atoms, which has been shown to be a working principle in zinc and cadmium complexes of the formula $[M(MR)_4(ONR'_2)_6]$ (M = Zn,[6] Cd;[7] R = Me, Et, *i*Pr etc.). It is also possible to introduce hydroxylaminato ligands into group 4 transition metal chemistry as shown for Ti^{4+}, which can adopt an unexpectedly high coordination number of eight if surrounded by hydroxylaminato ligands, as has been demonstrated for $[Ti(ONR_2)_4]$ (R = Me,[1c] Et[1d]). The flexibility of coordination in such hydroxylaminato complexes has also been used to design hemilabile half-sandwich polymerisation catalysts.[1a,1e] The principle of achieving unusually high coordination numbers has impressively been demonstrated by Batten and Deacon et al., who have shown the ability of nitroso ligands to lead to extremely high coordination numbers of up to twelve in rare-earth metal complexes.[8]

We have recently started exploring the chemistry of hydroxylaminato complexes of rare-earth metals. As hydroxylaminato ligands can exert an η^2-binding mode towards rare-earth metal atoms a saturation of these large metal ions coordination sphere can be accomplished by a minimum of atoms, and thus no long spacer groups are necessary as it is normally the case for many neutral-donor-functionalised ligands.

[a] Anorganische Chemie und Strukturchemie, Universität Bielefeld, Universitätsstraße 25, 33615 Bielefeld, Germany
Fax: +49-521-106-6182
E-mail: mitzel@uni-bielefeld.de
http://www.uni-bielefeld.de/chemie/ac3/ak-mitzel/start.html
Supporting information for this article is available on the WWW under http://dx.doi.org/10.1002/ejic.201000121.

Our investigations are focusing on the reactions of *N*,*N*-dialkylated hydroxylamines with different rare-earth metal precursors and compounds. Combining cyclopentadienide substituents with hydroxylaminato-κO ligands leads to a variety of complexes with different binding and aggregation modes. With larger N-substituents like the benzyl group, we have demonstrated that compounds like [Cp$_2$Y(ONBn$_2$)]$_2$ and [Cp$_2$Sm(ONBn$_2$)]$_2$ form dimers, which have the hydroxylaminato ligands binding side-on but also linking the metal atoms by oxygen donors into four-membered ring systems.[9] A trinuclear compound [Cp$_5$Y$_3${ON(Me)CH$_2$-CH$_2$(Me)NO}$_2$] was obtained by the reaction of YCp$_3$ and the bishydroxylamine HON(Me)CH$_2$CH$_2$(Me)NOH and shows the same combination of binding modes.[9] The application of *N*,*N*-dialkylhydroxylamine anions, preferably in the form of potassium salts, with small substituents in the absence of other groups at the rare-earth metal atoms leads exclusively to the formation of ate complexes, which aggregate into polymeric chain structures in the solid state.[10,11] Single-pot salt metathesis reactions involving the anhydrous rare-earth metal trichlorides LnCl$_3$ (Ln = Y, Ho, Er and Lu) and the *N*,*N*-diethylhydroxylaminato potassium salt KONEt$_2$ as well as KC$_5$Me$_5$ have resulted in the formation of a series of isostructural rare-earth metal hydroxylaminato complexes of the type [(C$_5$Me$_5$)Ln(μ-η^1:η^2-ONEt$_2$)(η^2-ONEt$_2$)]$_2$ (Ln = Y, Ho, Er and Lu). These have – analogously to above cases – similar bridging and side-on binding *N*,*N*-diethylhydroxylaminato ligands, but also one of these ligands per metal atom with a pure side-on binding mode.[11,12] Before these investigations by our group, only one hydroxylamine related complex has been reported.[13] This compound, [{(C$_5$H$_6$Me$_4$NO)$_2$Sm(μ-ONC$_5$H$_6$Me$_4$)}$_2$], contains hydroxylaminato-κO ligands binding end-on and μ-O-side-on in one complex introduced by the stable TEMPO radical in a redox process.

Recently we reported the possibility generating the first monomeric hydroxylaminato rare-earth metal complexes [Cp$_2$Ln{η^2-ON(C$_2$H$_4$-η^1-*o*-Py)(C$_2$H$_4$-*o*-Py)}] with the *N*,*N*-bis(2-{pyrid-2-yl}ethyl)hydroxylaminato ligand.[14] With this ligand system the coordination of one pyridine donor atom effects that a dimerisation via an Ln$_2$O$_2$ linkage is disfavoured. Also the molecular structures, ligand coordination modes and aggregation types of these complexes depend strongly on the ionic radii of the involved rare-earth metal ions. For the smaller metal ions (Sm^{3+}, Y^{3+}) a monomeric motif is fond for the Cp$_2$Ln complexes of this ligand (Type A, Scheme 1). If rare-earth metal ions with larger ionic radii than that of Sm^{3+} (Nd, Pr) were employed in syntheses, the molecular structures reveal the well known dimeric μ-O-bridging motif without coordination of a pyridine donor (Type B, Scheme 1) as we previously observed e.g. in [Cp$_2$Y(ONBn$_2$)]$_2$.[9] Utilising the even larger lanthanum leads to the additional coordination of a pyridine donor atom and increases the coordination number of the metal ion by one (Type C, Scheme 1). The donor-stabilised complexes are hemilabile and change their coordination rapidly in solution. In order to investigate the hemilability we tried to occupy the free pyridine donor-site with Lewis acids to block such exchange processes. Here we present the formation of complexes resulting from the interactions of the Lewis-acidic metal trialkyls EMe$_3$ (E = Al, Ga, In) with these [Cp$_2$LnON(C$_2$H$_4$-*o*-Py)$_2$] complexes revealing novel aggregation motifs and different aggregation in solution.

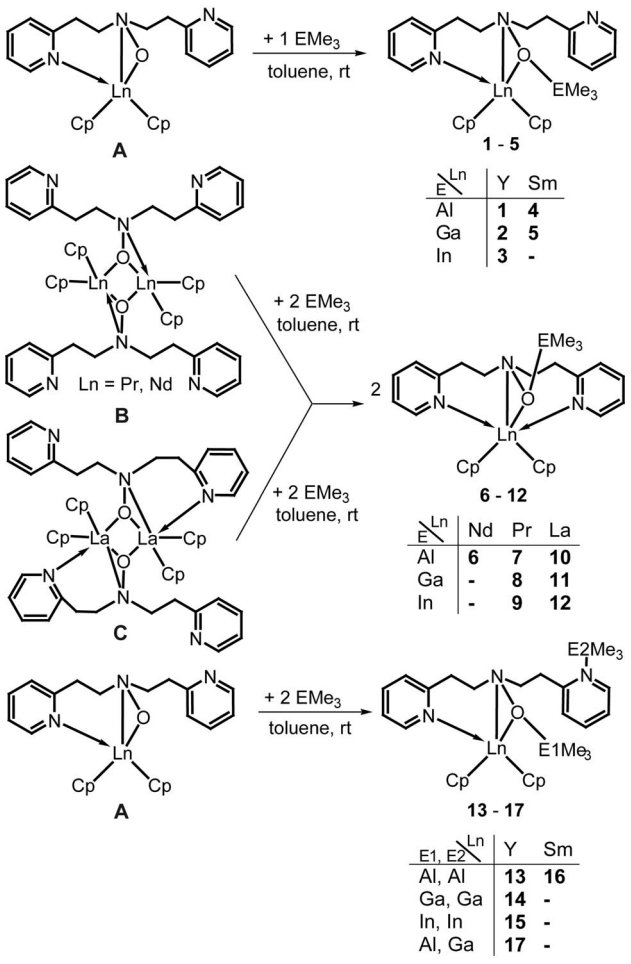

Scheme 1. Synthetic routes to the adduct complexes **1**–**17** starting from the monomeric compounds [Cp$_2$Ln{η^2-ON(C$_2$H$_4$-η^1-*o*-Py)(C$_2$H$_4$-*o*-Py)}] (Ln = Y, Sm), the dimeric compounds [Cp$_2$Ln{η^2-ON(C$_2$H$_4$-*o*-Py)$_2$}] (Ln = Nd, Pr) and the dimeric lanthanum complex [Cp$_2$La{η^2-ON(C$_2$H$_4$-η^1-*o*-Py)(C$_2$H$_4$-*o*-Py)}]$_2$.

Results and Discussion

Synthesis and Characteristics of the EMe$_3$ Adducts of [Cp$_2$Ln{η^2-ON(C$_2$H$_4$-*o*-Py)$_2$}]

Based on the complexes [Cp$_2$Ln{η^2-ON(C$_2$H$_4$-*o*-Py)$_2$}], which are accessible via a hydrocarbon elimination route by reacting LnCp$_3$ with HON(C$_2$H$_4$-*o*-Py)$_2$ in thf,[14] complexes **1**–**17** were synthesised by reacting them with pure AlMe$_3$, GaMe$_3$ and InMe$_3$. This resulted in a variety of ligand binding and aggregation modes. As starting materials and products in these syntheses decompose upon contact with oxygen and/or moisture the preparative protocol dictates a rigorous exclusion of traces of the atmosphere.

To achieve the formation of the compounds **1**–**12** the complexes [$Cp_2Ln\{\eta^2$-$ON(C_2H_4$-*o*-$Py)_2\}$] (Cp = cyclopentadienyl, Py = pyridyl, Ln = Y, Sm, Nd, Pr, La) were suspended in toluene and *equimolar* amounts of pure EMe_3 (E = Al, Ga, In) were added (Scheme 1).

In related reactions the complexes **13**–**16** were synthesised by reacting the starting materials with two equivalents of the Lewis acids. Compound **17** is accessible by treating compound **1** with 1.1 equiv. of $GaMe_3$ in toluene. Complexes **1**–**12** are of superior solubility in toluene in contrast to the utilised starting materials [$LnCp_2$-η^2-$ON(C_2H_4$-*o*-$Py)_2$]. Addition of a second equivalent of the Lewis acids further improves the solubility of the products. Yields of these syntheses were up to 88% and all synthesised complexes have colours typical for the utilised lanthanide. The proof of identity stems from CHN analyses, NMR spectra (where applicable) and single-crystal X-ray diffraction experiments. We expect that it is possible to perform these syntheses across the whole rare-earth series no matter if a monomeric starting material is used or the dimeric types. As the matrix of all possible combinations of rare-earth metals and $AlMe_3$, $GaMe_3$ or $InMe_3$ and their combinations could contain up to 70 entries, we decided to investigate only one member of each of the three known structural motifs of the starting materials and chose the lanthanum, praseodymium and yttrium compounds for this purpose. In addition we synthesised a few complexes of samarium and neodymium to check for the validity of our similarity assumptions.

Molecular Structures of the Complexes [$Cp_2LnON(C_2H_4$-*o*-$Py)_2$·EMe_3] 1–12

The results of the structural analyses of compounds **1**–**12** can be grouped into two structural motifs (see

Table 1. Selected structural parameters for compounds **1**–**17** as determined by X-ray crystallography (av. = average value).

	1 Ln = Y, E = Al	**2** Ln = Y, E = Ga	**3** Ln = Y, E = In	**4** Ln = Sm, E = Al	**5** Ln = Sm, E = Ga	**6** Ln = Nd, E = In	**7** Ln = Pr, E = Al	**8** Ln = Pr, E = Ga	**9** Ln = Pr, E = In	**10** Ln = La, E = Al
Ln(1)–O(1)	2.234(2)	2.216(2)	2.200(2)	2.302(1)	2.272(2)	2.351(1)	2.405(1)	2.370(2)	2.357(2)	2.499(1)
Ln(1)–N(1)	2.512(3)	2.508(2)	2.509(3)	2.556(1)	2.537(3)	2.545(2)	2.537(2)	2.529(2)	2.548(2)	2.628(2)
Ln(1)–N(2)	2.444(3)	2.445(2)	2.446(3)	2.509(2)	2.510(3)	2.696(2)	2.724(2)	2.730(2)	2.707(2)	2.739(2)
Ln(1)–N(3)	–	–	–	–	–	2.729(2)	2.726(2)	2.723(2)	2.737(2)	2.768(2)
Ln(1)–C(1–10)	$2.675_{av.}$	$2.693_{av.}$	$2.690_{av.}$	$2.733_{av.}$	$2.766_{av.}$	$2.819_{av.}$	$2.822_{av.}$	$2.832_{av.}$	$2.829_{av.}$	$2.859_{av.}$
O(1)–N(1)	1.454(4)	1.452(2)	1.453(3)	1.451(2)	1.454(4)	1.447(2)	1.450(2)	1.445(3)	1.445(2)	1.449(2)
O(1)–E(1)	1.877(3)	2.051(2)	2.264(2)	1.886(1)	2.036(2)	2.262(1)	1.888(2)	2.036(2)	2.261(1)	1.882(2)
N(1)–C(11)	1.475(4)	1.484(3)	1.476(4)	1.475(2)	1.471(4)	1.484(2)	1.488(3)	1.488(3)	1.478(3)	1.476(3)
N(1)–C(18)	1.477(5)	1.476(3)	1.482(4)	1.477(2)	1.473(4)	1.479(2)	1.478(3)	1.478(3)	1.477(2)	1.483(3)
O(1)–Ln(1)–N(1)	35.1(1)	35.1(1)	35.2(1)	34.2(1)	34.6(1)	34.1(1)	34.0(1)	34.1(1)	34.0(1)	32.7(1)
O(1)–Ln(1)–N(2)	102.4(1)	102.5(1)	102.2(1)	101.1(1)	101.5(1)	86.3(1)	85.4(1)	85.0(1)	86.2(1)	88.4(1)
N(1)–Ln(1)–N(2)	76.2(1)	76.6(1)	76.7(1)	75.7(1)	75.7(1)	75.7(1)	75.4(1)	75.3(1)	75.3(1)	75.5(1)
N(2)–Ln(1)–N(3)	–	–	–	–	–	155.0(1)	152.5(1)	152.9(1)	154.7(1)	154.3(1)
N(1)–O(1)–Ln(1)	83.0(2)	83.5(1)	84.1(2)	82.5(1)	82.7(2)	80.3(1)	78.0(1)	79.0(1)	80.3(1)	78.5(1)
E(1)–O(1)–Ln(1)	145.6(1)	145.7(1)	145.7(2)	144.5(1)	145.5(1)	151.4(1)	154.6(1)	154.9(1)	151.3(1)	153.8(1)
E(1)–O(1)–N(1)	131.2(2)	130.6(1)	130.2(2)	132.7(2)	131.6(2)	128.3(1)	127.2(1)	125.7(2)	128.4(1)	127.3(2)
O(1)–N(1)–Ln(1)	62.0(1)	61.4(1)	60.7(1)	63.2(1)	62.7(2)	65.6(1)	68.0(1)	66.9(1)	65.7(1)	68.8(1)

	11 Ln = La, E = Ga	**12** Ln = La, E = In	**13** Ln = Y, E = Al	**14** Ln = Y, E = Ga	**15** Ln = Y, E = In	**16** Ln = Sm, E = Al	**17** Ln = Y, E(1) = Al E(2) = Ga
Ln(1)–O(1)	2.413(2)	2.407(1)	2.250(4)	2.218(3)	2.206(4)	2.306(3)	2.246(3)
Ln(1)–N(1)	2.612(3)	2.588(2)	2.503(5)	2.472(4)	2.506(5)	2.540(3)	2.501(4)
Ln(1)–N(2)	2.760(3)	2.733(2)	2.475(5)	2.475(3)	2.463(5)	2.519(3)	2.455(4)
Ln(1)–N(3)	2.765(3)	2.759(2)	–	–	–	–	–
Ln(1)–C(1–10)	$2.875_{av.}$	$2.875_{av.}$	$2.683_{av.}$	$2.684_{av.}$	$2.683_{av.}$	$2.7013_{av.}$	$2.680_{av.}$
O(1)–N(1)	1.448(3)	1.445(2)	1.464(6)	1.449(4)	1.455(6)	1.453(4)	1.458(5)
O(1)–E(1)	2.046(2)	2.254(1)	1.883(5)	2.038(3)	2.267(4)	1.887(3)	1.924(3)
N(3)–E(2)	–	–	2.028(5)	2.133(3)	2.409(6)	2.040(3)	2.136(4)
N(1)–C(11)	1.483(4)	1.481(2)	1.463(8)	1.471(5)	1.476(8)	1.471(5)	1.471(6)
N(1)–C(18)	1.488(4)	1.474(2)	1.474(8)	1.471(5)	1.469(8)	1.484(5)	1.486(6)
O(1)–Ln(1)–N(1)	33.2(1)	33.4(1)	35.4(2)	35.5(1)	35.2(2)	34.5(1)	35.2(2)
O(1)–Ln(1)–N(2)	86.7(1)	86.3(1)	102.5(2)	102.9(2)	104.1(2)	102.4(1)	103.7(1)
N(1)–Ln(1)–N(2)	74.4(1)	75.0(1)	74.7(2)	75.3(1)	75.0(1)	75.2(1)	76.1(1)
N(2)–Ln(1)–N(3)	152.2(1)	153.8(1)	–	–	–	–	–
N(1)–O(1)–Ln(1)	81.0(2)	80.2(1)	81.8(3)	81.9(2)	83.7(3)	81.6(2)	82.0(2)
E(1)–O(1)–Ln(1)	151.2(1)	151.4(1)	148.5(2)	148.7(2)	144.3(2)	146.3(2)	147.0(2)
E(1)–O(1)–N(1)	127.9(2)	128.3(1)	128.9(3)	128.2(2)	132.0(3)	131.5(2)	130.3(2)
O(1)–N(1)–Ln(1)	65.8(2)	66.4(1)	62.8(2)	62.7(2)	61.1(2)	63.9(1)	62.8(2)
E(2)–N(3)–C(20)			125.2(4)	124.1(3)	131.9(4)	123.8(2)	123.9(3)
E(2)–N(3)–C(24)			117.3(5)	117.0(3)	110.5(4)	116.8(3)	116.5(3)

Scheme 1), which will be discussed in the following paragraph. They show that the radius of the metal atom is the critical parameter for changing between coordination and aggregation modes of the ligand and complexes, respectively. For comparison the values of bond lengths and bond angles of all compounds are listed in Table 1.

Molecular Structures of the Complexes [Cp$_2$LnON(C$_2$H$_4$-o-Py)$_2$·EMe$_3$] 1–5

Rare-earth metal atoms with comparatively small ionic radii and one EMe$_3$ unit are contained in the adduct complexes **1** (Ln = Y^{3+}, E = Al^{3+}), **2** (Ln = Y^{3+}, E = Ga^{3+}), **3** (Ln = Y^{3+}, E = In^{3+}), **4** (Ln = Sm^{3+}, E = Al^{3+}) and **5** (Ln = Sm^{3+}, E = Ga^{3+}). This group of complexes represents the first structural type. For these, the X-ray diffraction analyses reveal a monomeric structural motif were the hydroxylaminato function forms an N(1)–O(1)–Ln(1) ring by interacting with the rare-earth metal atom in an η^2-fashion. Furthermore, one nitrogen donor atom, N(2), of the two pyridine fragments coordinates to the rare-earth metal atom, while the other one, N(3), remains non-bonded. This coordination leads to a six-membered Ln(1)–N(1)–C(11)–C(12)–C(13)–N(2) ring adopting a boat conformation. Moreover two cyclopentadienyl rings are η^5-bondend to the rare-earth metal atom. The metal atom coordinates via a strong dative contact from the hydroxylaminato oxygen atom. As these five complexes are isostructural, only the structure of [Cp$_2$YON(C$_2$H$_4$-*o*-Py)$_2$·AlMe$_3$] (**1**) is presented in Figure 1.

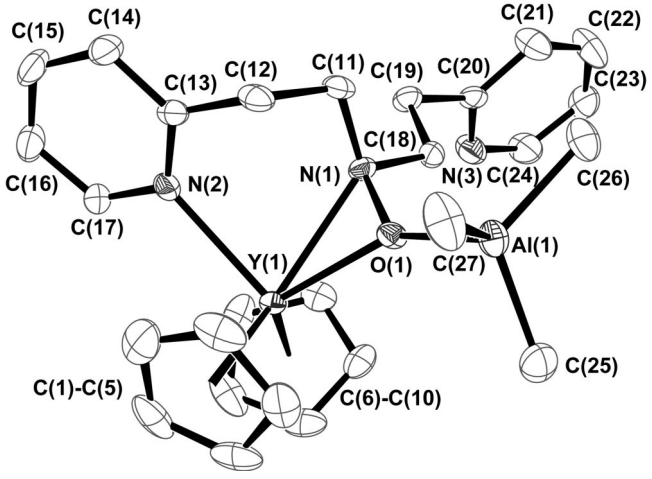

Figure 1. Molecular structure of [Cp$_2$YON(C$_2$H$_4$-*o*-Py)$_2$·AlMe$_3$] (**1**). Ellipsoids show 50% probability levels and hydrogen atoms have been omitted for clarity. Selected distances [Å]: O(1)–Al(1) 1.887(3), Y(1)–O(1) 2.234(2), Y(1)–N(1) 2.512(3) Y(1)–N(2) 2.444(3). Selected angles in [°]: Al(1)–O(1)–Y(1) 145.6(1), Al(1)–O(1)–N(1) 131.2(2), O(1)–Y(1)–N(1) 35.1(1), O(1)–Y(1)–N(2) 102.4(1), N(1)–Y(1)–N(2) 76.2(1).

We shall now discuss the structure of complex **1** in more detail and compare it to relevant compounds in the literature. Following this, the structures of complexes **1**–**5** will be compared among each other.

The donating hydroxylaminato oxygen atom forms a dative O(1)–Al(1) bond towards the aluminium atom with a length of 1.887(3) Å. This O–Al distance, compared to literature values of other AlMe$_3$-oxygen adducts like OMe$_2$·AlMe$_3$ [1.939(2) Å],[15] 18-crown-6·4AlMe$_3$ [1.985(6) Å],[16] bis(trimethylaluminium)-1,4-dioxane [2.02(2) Å[17]] or the bridging [tris(μ$_2$-butoxo-μ$_2$-methyl-dimethylaluminate)yttrium(III)] [1.864(20) Å],[18] can be interpreted as a strong dative bond, especially considered, that the oxygen atom is located next to two electropositive metal atoms, namely yttrium and aluminium, which have to share the electronic density located at the oxygen atom.

The distances of the hydroxylaminato-metal atoms in complex **1**, O(1)–Y(1) and N(1)–Y(1) at 2.234(2) and 2.512(3) Å, are significantly longer than those in the non-substituted complex [Cp$_2$YON(C$_2$H$_4$-*o*-Py)$_2$] with values for O(1)–Y(1) at 2.172(2) and N(1)–Y(1) at 2.437(2) Å,[14] but nearly in the same range as in the complex [{Cp$_2$Y-(ONBn)$_2$}$_2$] [O(1)–Y(1) 2.248(3), N(1)–Y(1) 2.503(3) Å], which contains a bridging hydroxylaminato function.[9] The donating pyridine fragment in **1** interacts via a short N(2)–Y(1) bond [2.444(3) Å]. This is 0.03 Å shorter than in the AlMe$_3$-free molecule [Cp$_2$YON(C$_2$H$_4$-*o*-Py)$_2$] and is in agreement with the lager values of the hydroxylaminato-ligand to metal contacts. Despite the strong O–Al interaction we observe nearly the same hydroxylaminato N–O distance for **1** [1.454(4) Å] as in HON(C$_2$H$_4$-*o*-Py)$_2$ [1.450(2) Å][19] or in *N*,*N*-dimethylhydroxylamine [1.452(2) Å].[20] The N(1)–O(1)–Y(1) ring exhibits bond angles O(1)–Y(1)–N(1) at 35.1(1)°, N(1)–O(1)–Y(1) at 83.0(2)° and O(1)–N(1)–Y(1) at 62.0(1)°. The N(1)–Y(1)–N(2) chelating angle is 76.2(1)°, which is 3.2° smaller than in [Cp$_2$YON(C$_2$H$_4$-*o*-Py)$_2$]. Together with the values for the angles Al(1)–O(1)–Y(1) at 145.6(2)° and Al(1)–O(1)–N(1) at 131.2(2)° the coordination geometry at O(1) has to be described as trigonal planar, distorted by the three-membered N(1)–O(1)–Y(1) ring.

Examining the structural parameters of compounds **2** and **3** reveals a major influence of the earth metal atom on the bond lengths in the structures. The weaker Lewis acid GaMe$_3$ in complex **2** leads to an O(1)–Ga(1) contact of 2.051(2) Å, which is 0.16 Å larger than the O(1)–Al(1) bond in complex **1**. This leads to a shortening of the O(1)–Y(1) bond [2.216(2) Å] by 0.018 Å relative to **1**.

This shortening effect is even more pronounced when InMe$_3$ acts as the Lewis acid in complex **3**. The indium atom coordinates to the hydroxylaminato oxygen atom, similar to **1** and **2**, and the O(1)–In(1) bond has a length of 2.264(2) Å, i.e. 0.38 Å longer than the corresponding one of **1** and 0.21 Å longer than that in **2**. Consequently, the O(1)–Y(1) distance in complex **3** at 2.200(2) Å is 0.034 Å shorter than in complex **1** and 0.016 Å shorter than in complex **2**. Thus the length of the O(1)–Y(1) bond in the present cases **1** to **3** represents an indicator of the Lewis acidity of AlMe$_3$, GaMe$_3$ and InMe$_3$ with the advantage of not taking the ionic-radius of the Lewis acids into account. Interestingly the formation of the adducts has no influence on the N(1)–Y(1) and the N(2)–Y(1) bonds, which stay almost constant in the complexes **1**–**3**. Compared to the five reported literature compounds in the CCDC-database for

dative O–Ga bonds the O(1)–Ga(1) bond in complex **2** can be handled as a strong interaction. For example the ether adducts $Me_2O{\cdot}GaMe_3$ and bis(trimethylgallium)(dibenzo-16-crown-6) exhibit considerably longer O–Ga distances at 2.155(2)[15] and 2.198(8) Å,[21] respectively.

The utilisation of Sm^{3+}, as represented in the structures of compounds **4** and **5**, leads to analogous results. In complex **4** the Al–O bond has a length of 1.886(1) Å, which is of the same dimension as in **1**. The gallium analogue **5** exhibits an O(1)–Ga(1) bond with a length of 2.036(2) Å, which is the shortest $GaMe_3$–oxygen dative bond reported so far. As well as in **1**–**3** the O(1)–Y(1) bonds in **4** and **5** are shortened in dependency of the Lewis acid. For a more detailed comparison of bond lengths and angles of the samarium complexes see Table 1.

Molecular Structures of the Complexes [$Cp_2LnON(C_2H_4$-o-Py)$_2{\cdot}EMe_3$] 6–12

Complexes **6**–**12** contain the early lanthanide elements Nd, Pr and La and represent the second structural type. The main difference by comparing the Nd and Pr compounds **6**–**9** with the La compounds **10**–**12** is, that despite all have the same structure type, their precursor complexes have not. In contrast to the Nd and Pr precursors, the lanthanum precursor [{$LaCp_2ON(C_2H_4$-*o*-Py$)_2$}$_2$], has one pyridine fragment coordinated to the rare-earth metal atom (see Scheme 1). The interaction of the EMe_3 unit with the precursors does not only deaggregate them, but by blocking the oxygen donor site gives room for coordination of both pyridine donors.

We found three different unit cells for the crystals of the group of complexes **6**–**12**, but as the structural values and the coordination are very similar, only complex **9** is presented in Figure 2 and mainly this will be described in more detail as a representative of the group.

The coordination mode of the *N*,*N*-bis{2-(pyrid-2-yl)-ethyl}hydroxylaminato ligand, which uses both pyridine donors and its ON unit in an η^2-mode to bind to one metal atom has previously been reported by Ziegler et al. for a chromium(III) chloride complex.[22] This coordination mode in **6**–**12** leads to two six-membered Ln–N–C–C–C–N rings adopting a strongly distorted boat conformation.

The Lewis acid EMe_3 coordinates via a strong dative contact from the hydroxylaminato oxygen atom as observed for complexes **1**–**5**. Compared to the dimeric precursor complexes of complexes **6**–**12** without EMe_3 units (see Scheme 1), the coordination of these Lewis acids forces complexes **6**–**12** to be monomeric. The adduct formation at oxygen prohibits the dimerisation through a bridging hydroxylaminato oxygen atom. Due to this, the contact of the Lewis acids EMe_3 leads to a higher coordination number in the case of praseodymium and neodymium than observed in their precursor complexes (Scheme 1), wherein none of the nitrogen donor atoms coordinates to the rare-earth metal atom. This underlines the sensitivity of the binding situation at the rare-earth metal atom, which undergoes intense changes by formation of a dative contact to EMe_3.

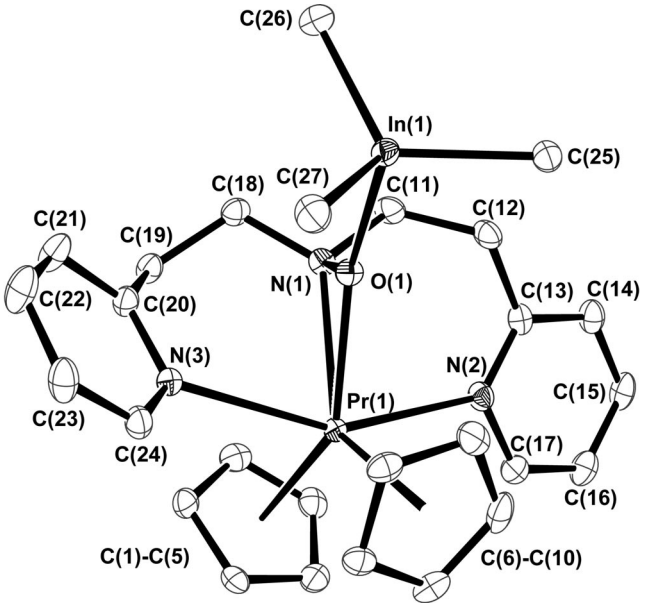

Figure 2. Molecular structure of [$Cp_2PrON(C_2H_4$-*o*-Py$)_2{\cdot}InMe_3$] (**9**). Ellipsoids show 50% probability levels and hydrogen atoms have been omitted for clarity. Selected distances [Å]: O(1)–In(1) 2.261(1), Pr(1)–O(1) 2.357(2), Pr(1)–N(1) 2.548(2), Pr(1)–N(2) 2.707(2), Pr(1)–N(3) 2.737(2). Selected angles in [°]: In(1)–O(1)–Pr(1) 151.3(1), In(1)–O(1)–N(1) 128.4(1), O(1)–Pr(1)–N(1) 34.0(1), O(1)–Pr(1)–N(2) 86.2(1), N(1)–Pr(1)–N(2) 75.3(1), N(2)–Pr(1)–N(3) 154.7(1).

The indium atom In(1) coordinates to the oxygen atom and forms a dative O(1)–In(1) bond with a distance of 2.261(1) Å. This value is of the same range as for complex **3** and is – compared to the only known literature complex containing a dative $InMe_3$–oxygen bond in the CCDC database with an O–In distance of 2.261(3) Å[23] – again a strong interaction. Further comparisons with the tris(mesityl)indium-tetrahydrofuran adduct or the tris(3,3,3-trifluoropropynyl)indium-bis(tetrahydrofuran) adduct with O–In distances of 2.414[24] and 2.300(8) Å,[25] respectively, underline this statement. The O(1)–Pr(1) bond of complex **9** at 2.357(2) Å is 0.157 Å longer than in complex **3**, whereas the N(1)–Pr(1) bond at 2.548(3) Å is only widened by 0.039 Å indicating a more side-on coordination type of the hydroxylaminato function in compound **9**. In contrast to complexes **1**–**5** these bonds are shorter than those in the $InMe_3$-free complex [{$Cp_2PrON(C_2H_4$-*o*-Py$)_2$}$_2$] with values for O(1)–Pr(1) at 2.375(1) and N(1)–Pr(1) at 2.575(1) Å; this is obviously due to the changed μ-O binding situation in [{$Cp_2PrON(C_2H_4$-*o*-Py$)_2$}$_2$].[14]

The N(1)–O(1) distance in **9** is 1.445(2) Å and similar to the N–O bonds in **1**–**5**. The N(1)–O(1)–Pr(1) ring exhibits three bond angles O(1)–Pr(1)–N(1) at 34.0(1)°, N(1)–O(1)–Pr(1) at 80.3(1)° and O(1)–N(1)–Pr(1) at 65.7(1)°. The angle at the hydroxylaminato oxygen In(1)–O(1)–Pr(1) is 151.3(1)° and for In(1)–O(1)–N(1) a value of 128.4(1)° is observed. Together with the N(1)–O(1)–Pr(1) angle mentioned above this adds up to exactly 360°, indicating planarity at the oxygen atom.

The bonding of the pyridine units can be characterised by the angles N(1)–Pr(1)–N(2) [75.3(1)°] and N(2)–Pr(1)–N(3) [154.7(1)°]. The pyridine–metal bonds N(2)–Pr(1) and N(3)–Pr(1) have lengths of 2.707(2) and 2.737(2) Å, respectively. Taking the differences of the ionic radii into account, these interactions appear to be weaker than in the group of compounds **1**–**5**. This is obviously due to a higher coordination number at the rare-earth metal atom.

The interaction of $AlMe_3$ leads to O(1)–Al(1) distances of 1.888(2) in complex **7** and 1.882(2) Å in compound **10**, which is in the same range as the observed distances in complexes **1** and **4**. Also for the interaction of $GaMe_3$ (**8**, **11**) and $InMe_3$ (**6**, **9**, **12**) the O–E values change only marginally compared to the corresponding structures of the first complex group **1**–**5**. By coordination of the Lewis acids EMe_3 to the hydroxylaminato oxygen atom the O(1)–Ln(1) bonds get shortened to an extent dependent on the Lewis acidity of the EMe_3 units. The shortest O(1)–Ln(1) bond is observed for the neodymium complex upon interaction with $InMe_3$ (**6**) with a value of 2.351(1) Å. The longest bond is found in the lanthanum containing complex **10** with coordinated $AlMe_3$, in which the O(1)–Ln(1) distance is 2.499(1) Å. Compared to the larger variations of the Ln–O bonds upon coordination of the EMe_3 units to oxygen atoms, the Ln–N bonds are almost unaltered. The values change according to the ionic radii of the rare-earth metal atoms and lie between 2.529(2) and 2.628(2) Å for the N(1)–Ln(1) bond and between 2.696(1) and 2.768(2) Å for the N(2)–Ln(1) and N(3)–Ln(1) bonds, respectively. Only the lanthanum containing complexes **10**–**12** form a series where the N(1)–La(1) distance undergoes a shortening similar to the O(1)–Ln(1) bond in the series $AlMe_3$ (**10**) $GaMe_3$ (**11**) and $InMe_3$ (**12**).

Molecular Structures of the Complexes $[Cp_2LnON(C_2H_4$-*o*-$Py)_2{\cdot}2EMe_3]$ 13–17

The complexes of rare-earth metals with comparatively small ionic radii can also interact with two EMe_3 Lewis acids. The resulting complexes are **13** (Ln = Y^{3+}, E = Al^{3+}), **14** (Ln = Y^{3+}, E = Ga^{3+}), **15** (Ln = Y^{3+}, E = In^{3+}), **16** (Ln = Sm^{3+}, E = Al^{3+}) and **17** [Ln = Y^{3+}, E(1) = Al^{3+}, E(2) = Ga^{3+}]. The crystal structure analyses reveal a common monomeric structural motif. The hydroxylaminato ligand coordinates in an ON–η^2-fashion to the rare-earth metal atoms. In addition, one Lewis acid EMe_3 interacts with the hydroxylaminato oxygen atom whereas the second EMe_3 unit coordinates to a pyridine nitrogen donor site N(3). The remaining nitrogen donor atom N(2) coordinates to the rare-earth metal atom. As in complexes **1**–**12**, this coordination of N(2) leads to a six-membered Ln(1)–N(1)–C(11)–C(12)–C(13)–N(2) ring adopting a distorted boat conformation. Two η^5-bonded cyclopentadienyl rings complete the coordination sphere of the Ln atom.

As the five complexes **13**–**17** are isostructural, the structure of only the heterotrimetallic compound **17**, containing yttrium, aluminium and gallium in one complex is presented in Figure 3 and will be discussed in detail as a representative.

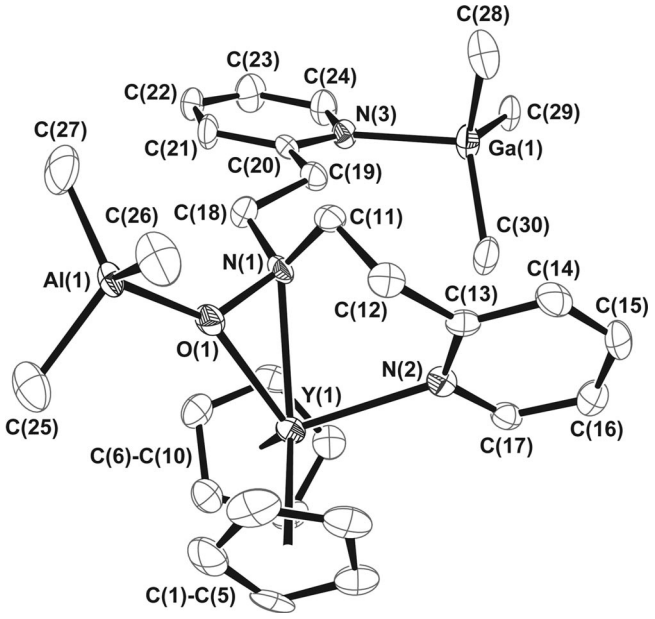

Figure 3. Molecular structure of $[Cp_2YON(C_2H_4$-*o*-$Py)_2{\cdot}AlMe_3{\cdot}GaMe_3]$ (**17**). Ellipsoids show 50% probability levels and hydrogen atoms have been omitted for clarity. Selected distances [Å]: O(1)–Al(1) 1.924(3), N(3)–Ga(1) 2.136(4), Y(1)–O(1) 2.246(3), Y(1)–N(1) 2.501(4) Y(1)–N(2) 2.455(4). Selected angles in [°]: Al(1)–O(1)–Y(1) 147.0(2), Al(1)–O(1)–N(1) 130.3(2), O(1)–Y(1)–N(1) 35.2(2), O(1)–Y(1)–N(2) 103.7(1), N(1)–Y(1)–N(2) 76.1(1).

The structure of compound **17** is similar to the aggregation in complexes **1**–**5** with the difference that the free pyridine donor atom N(3) interacts with $GaMe_3$ to form a N(3)–Ga(1) bond of 2.136(4) Å length. This value is in the same range as for known pyridine related gallium atom contacts like in [trimethylgallium-5,6-benzoquinoline] [2.152(3) Å[26]] or [trimethylgallium-4-(dimethylamino)pyridine] [2.085(2) Å[27]]. The $AlMe_3$ unit interacts with the oxygen atom and forms a dative O(1)–Al(1) bond of 1.924(3) Å length. This value is between 0.04–0.05 Å larger as in the aluminium containing complexes **1**, **4**, **7** and **10**. The oxygen to rare-earth metal bond of complex **17**, O(1)–Y(1) at 2.246(3) Å, and the N(1)–Y(1) bond at 2.501(4) Å show nearly the same lengths as in complex **1**. Examination of the bond angles at the hydroxylaminato oxygen atom indicates a strongly distorted trigonal, but planar arrangement at O(1) as in compound **1**.

N(2) forms a dative N(2)–Y(1) bond between the pyridine fragment and the rare-earth metal atom with a distance of 2.455(4) Å. The $GaMe_3$ unit is bonded to this pyridine ring slightly offset (by ca. 3°) from its expected position, as characterised by the angle Ga(1)–N(3)–C(20) at 123.9(3)° and the angle Ga(1)–N(3)–C(24) at 116.5(3)°.

The structures of compounds **13**–**16** reveal that the earth metal atoms in the EMe_3 units take a major influence on the bond lengths of the LnON fragment of the complexes. The two units of the Lewis acid $AlMe_3$ in complex **13** form

dative bonds to the available donor sites: O(1)–Al(1) at 1.883(5) and N(3)–Al(2) at 2.028(5) Å. The N–Al bond can be compared to those in the trimethylaluminium-(4-dimethylaminopyridine) adduct with a value of 2.016(2) Å[27] or to the *N*,*N*′-bis(trimethylaluminium)-4,4′-bipyridine adduct with bond lengths of 2.032(2).[28]

In complex **14** $GaMe_3$ was employed instead as Lewis acid leading to the corresponding coordination motif with bond lengths: O(1)–Ga(1) at 2.038(3) and N(3)–Ga(2) at 2.133(3) Å. The latter is very close to the N(3)–Ga(2) distance observed in complex **17**. Using $InMe_3$ as Lewis acid leads to complex **15**. This reveals bond lengths of 2.267(4) for the O(1)–In(1) bond and 2.409(6) for the N(3)–In(2) bond.

The same structural motif but with Sm and Al as the two underlying metals is realised in compound **16**. The structural parameters are mostly analogous to those of compounds **13**–**15**. The earth metal bond to the oxygen atom has a length of 1.887(3) Å. The N(3)–Al(2) bond has a length of 2.040(3) Å. For a more detailed comparison of bond lengths and angles of the complexes **13**–**17** refer to Table 1.

Molecular Dynamics of the Compounds 1–17

We have previously reported the exchange processes for the hemilabile hydroxylaminato-yttrium complex with the *N*,*N*-bis{2-(pyrid-2-yl)ethyl}hydroxylaminato ligand (Type A, Scheme 1).[14] These processes lead to very complex VT-NMR spectra and we found that besides an exchange of the pyridyl groups, further dynamic processes take place.

Upon contact with one equivalent of $AlMe_3$, $GaMe_3$ or $InMe_3$, complexes **1**–**5** stay hemilabile, which is in agreement with the molecular structures in the solid state (see Figure 1), showing the EMe_3 groups to be coordinating to the oxygen atom of the hydroxylaminato ligand. Under these conditions the dynamic exchange of the two pyridine sites – one Ln-bonded and one free – is still possible (Scheme 2).

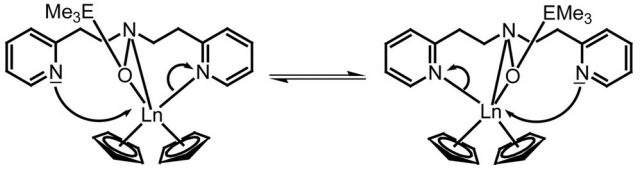

Scheme 2. Suggested dynamic exchange of the pyridyl functions in compounds **1**–**5** in solution.

The VT-NMR spectra of compound **2** (Ln = Y, E = Ga) provide evidence for this exchange. At room temp. the ^{1}H NMR spectra shows only one signal set, i.e. four signals for the eight aromatic protons, which means rapid exchange on the NMR time scale. Upon cooling to –80 °C a splitting of each aromatic signal is observed. This indicates that the dynamics can be frozen on the NMR time scale. A similar splitting is observed for the resonances of the cyclopentadienyl rings and the ethylene bridges. The singlet of the protons of $GaMe_3$ does not split into different signals, indicating that the gallium atom remains bonded to the hydroxylaminato oxygen atom during the exchange process. Compared to the spectra of the EMe_3-free [$YCp_2ON(C_2H_4$-*o*-$Py)_2$][14] (Type A) the coordination of the EMe_3-units to the ligand oxygen atom effects a simplification of the dynamic, because in this case solely the pyridyl exchange process and no further splitting is observed. By means of the Eyring equation it is possible to estimate the activation energy of this exchange process for **2** to be 44 kJ mol^{-1}.[29] **2** was chosen to be representative for the group of compounds **1**–**5**. Assorted NMR spectra of the complexes **1**–**5** including 2D NMR spectra are also collected in the Supporting Information to this paper.

Considering the structure motif of complexes **6**–**12** one could expect that these compounds have no ability to exchange because both pyridine rings are involved in the coordination to the rare-earth metal atom (see Figure 2). However the ^{1}H NMR experiment of compound **11**, a well suited representative for the series **6**–**12**, shows that these complexes undergo dynamic exchange processes at ambient temperature and the aromatic protons result in only one set of signals.

The VT-NMR spectra reveal a similar splitting at low temperature as observed for complexes **1**–**5**. This can be rationalised by assuming that the complexes have a different structure in solution, which is like that of the complexes **1**–**5**. The dynamic processes are thus those shown in Scheme 2. The fact that the activation energy at 44 kJ mol^{-1} is of the same dimension as for **1**–**5** underlines this statement.

Due to the presence of two different coordinated Lewis acids, $AlMe_3$ and $GaMe_3$, compound **17** exhibits the biggest potential to clarify the present dynamics. It was therefore chosen to represent the series of complexes **13**–**17**. The crystal structure of **17** shows, that one pyridine donor function is bonded to the yttrium atom and one bonded to the gallium atom. Expectedly, a pyridine exchange process as shown in Scheme 2 is not possible under these conditions. However, the VT-NMR experiments reveal, that complex **17** is hemilabile and has a striking dynamic behaviour. We therefore suggest a different dynamic exchange process for this complex and the related compounds, which is outlined in Scheme 3.

The VT-NMR spectra of compound **17** are presented in Figure 4. At 50 °C the eight protons of the two pyridine rings result in three signal groups. A doublet at δ = 8.51 ppm is observed caused by the protons labelled H2 in Figure 4. Next to this signal a triplet at δ = 7.74 ppm represents the protons H4. The signal of the protons H5 coincides with those of H3 resulting in a multiplet at δ = 7.25 ppm. Upon cooling the solution, the exchange process can be interrupted on the NMR time scale and the signals split into two different sets. One of these belongs to the pyridine ring coordinated yttrium atom, the other one to the pyridine ring coordinated to the gallium atom. The coalescence temperature T_C is –10 °C, which transforms into

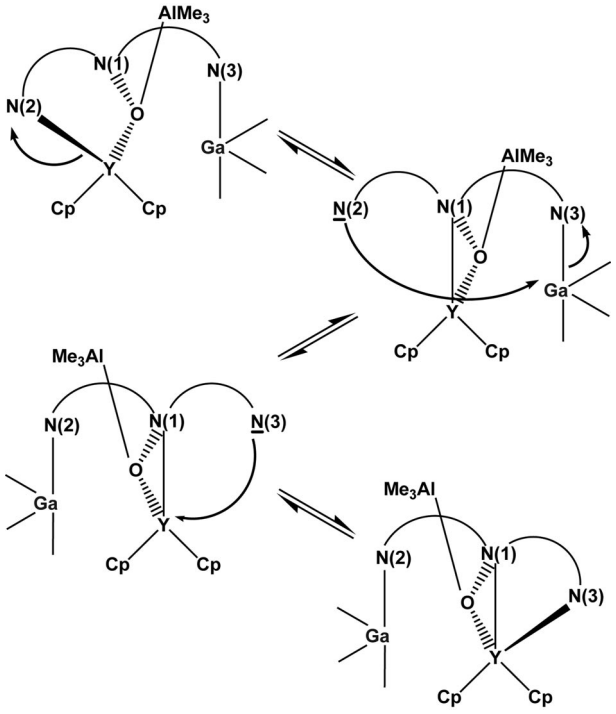

Scheme 3. Suggested dynamic exchange of the pyridyl rings at N(2) and N(3) in compounds **13**–**17**.

an energy barrier of 50 kJ mol^{-1}, which is 10 kJ mol^{-1} higher than in the precursor complex [YCp$_2$ON(C$_2$H$_4$-*o*-Py)$_2$] and 6 kJ mol^{-1} higher as for the mono adduct complexes **1**–**11**. In order to exclude that the NMR solvent [D$_8$]thf is involved in the dynamic processes we also measured a solution of complex **14** in [D$_8$]toluene. The spectra led to analogous results as for those in [D$_8$]thf, but here the coalescence temperature of the exchange process is at 30 °C which is 40 °C higher than in [D$_8$]thf. The calculated energy barrier in this case is 58 kJ mol^{-1}. This result evidences, that thf is not directly involved as a donor, but it promotes the exchange process probably by its higher polarity, thus lowering the energy barrier by 8 kJ mol^{-1}.

At –80 °C the NMR spectrum of complex **17** reveals eight well resolved signals for each aromatic proton. For example the signal of the H2 protons is split into two doublets at δ = 8.73 and 8.52 ppm. The doublet at δ = 8.73 ppm can be assigned to the H2 protons of the gallium-bonded pyridine ring. The doublet at δ = 8.52 ppm is assigned to the H2 protons of the yttrium-coordinated pyridine ring. The signals for the H3, H4 and H5 protons also show a splitting into two discrete signals at this temperature and all can be related to their belonging pyridine ring. At 50 °C the hydrogen atoms of the cyclopentadienyl rings give a singlet at δ = 6.09 ppm. This signal splits into two discrete singlets at –80 °C at δ = 6.35 and 6.04 ppm. Due to the coordination of the pyridyl functions to the metal atoms the eight protons of the ethylene bridge in complexes **1**–**5** and **12**–**17** exhibit an interesting twofold AA′BB′ spin system. As this assignment is extensive, complex and succeeded only in case of complex **14** is it not mentioned in detail at this place, but can be found in the Supporting Information.

An interesting observation is that neither the signal of the AlMe$_3$ unit nor the signal of GaMe$_3$ unit splits into different resonances upon cooling. This indicates that the AlMe$_3$ unit remains continuously bonded to the oxygen

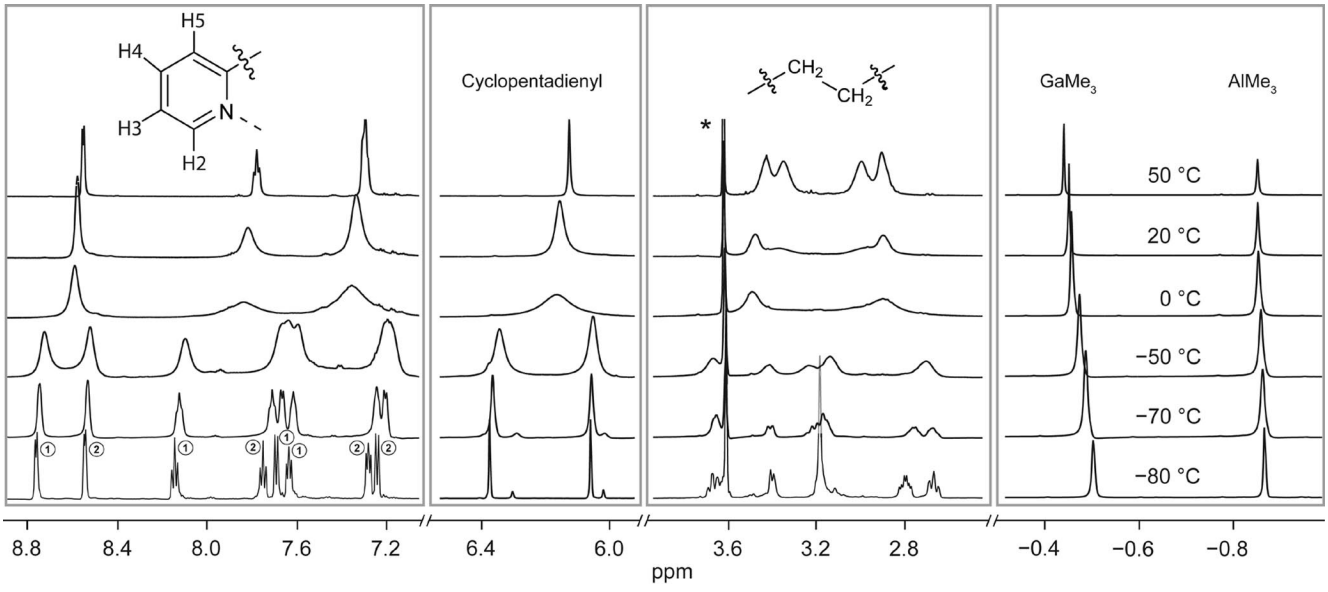

Figure 4. NMR spectra of compound **17** recorded between 50 °C and –80 °C. For clarity the Figure is split into different sections of the NMR spectra. They represent (left to right): the pyridyl-, the cyclopentadienyl-, the ethylene- and the earth-metal regions. No further peaks (except solvent residual peaks) were detected in the non-displayed regions. The sign circled 1 references the resonances of the protons of the gallium-bonded pyridine ring, circled 2 those of the yttrium-bonded pyridine ring.

atom, while the $GaMe_3$ unit exchanges between the two pyridyl groups. However, no exchange between the $AlMe_3$ and $GaMe_3$ units takes place. This verifies the mechanism suggested in Scheme 3.

As the adduct formation in complexes **13**–**16** occurs by the same Lewis acid, the observations in the VT-NMR spectra are obviously different. In these complexes the Lewis acid protons result in one sharp singlet a room and high temperature. At lower temperature this signal splits into two singlets – one for the nitrogen-bonded and one for the oxygen-bonded function. In these cases it is conceivable that the hydroxylaminato bonded Lewis acid can interfere in the exchange process. Further spectra of compound **13**–**17** including 2D NMR experiments are also collected in the Supporting Information.

Conclusions

We have shown that rare-earth metal complexes with donor-functionalised hydroxylaminato ligands exhibit a very sensitive ligand binding situation, which varies not only due to the different ionic radii of the rare-earth metal atoms, but also by interactions with Lewis acids like $AlMe_3$, $GaMe_3$ and $InMe_3$. The coordinating EMe_3 molecules block some of the donor sites of these complexes and thus inhibit further aggregation as observed in some of the underlying EMe_3-free complexes. Either only one of the pyridyl fragments of the *N*,*N*-bis(2-{pyrid-2-yl}ethyl)-hydroxylaminato ligands interacts with the rare-earth metal atom in the case of yttrium and samarium (**1–5**) or both pyridyl-nitrogen donor atoms complex the rare-earth metal atom as observed for the cases of neodymium, praseodymium and lanthanum (**6**–**12**). For the smaller rare-earth elements (here yttrium and samarium) it is also possible to generate double adducts of the complexes – either heterobimetallic (**13**–**16**) or heterotrimetallic (**17**). All compounds exhibit a pronounced dynamic behaviour in solution. For compounds **13**–**17**, where the free pyridine site is blocked by an EMe_3 unit, we suggest an exchange mechanism with only the pyridine-bonded EMe_3 unit being involved in the exchange.

Experimental Section

General Methods: All manipulations were performed under a rigorously dry inert atmosphere of argon using standard Schlenk and glove-box techniques. THF, toluene and *n*-pentane, dried with Na/benzophenone, were freshly condensed from $LiAlH_4$ before being employed in reactions. [D_8]THF was dried with Na/K alloy and degassed. MCp_3[30] and *N*,*N*-bis(2-{pyrid-2-yl}ethyl)hydroxylamine[19] were synthesised according to literature procedures. NMR measurements were undertaken with a Bruker Avance 400, a Bruker DRX 500 and a Bruker Avance 600. All NMR chemical shifts were referenced to the residual peaks of the protons of the used solvents. Elemental analyses were performed by using an Elementar Vario EL III CHNS and a Leco CHNS 932 instruments.

Crystallographic Structure Determinations: Single crystals suitable for X-ray diffraction measurement were picked inside a glove-box, suspended in a paratone-N/paraffin oil mixture, mounted on a glass fibre and transferred onto the goniometer of the diffractometer. The measurements were carried out with Mo-K_α radiation (λ = 0.71073 Å). The structures were solved by direct methods and refined by full-matrix least-squares cycles (program SHELX-97[31]). The structure-plot in this article were generated using the program ORTEP-III.[32] Crystallographic data (excluding structure factors) for the structures reported in this paper have been deposited with the Cambridge Crystallographic Data Centre as supplementary publications. The deposition numbers are provided in Table 2. These data can be obtained free of charge from The Cambridge Crystallographic Data Centre via www.ccdc.cam.ac.uk/data_request/cif.

General Procedure of the Mono Earth-Metal Alkyl Adducts [$Cp_2LnON(C_2H_4$-*o*-$Py)_2\cdot EMe_3$] (1–12): 0.5 mmol of recrystallised [$Cp_2LnON(C_2H_4$-*o*-$Py)_2$] (for Ln = Y, Sm) or 0.25 mmol [$Cp_2LnON(C_2H_4$-*o*-$Py)_2]_2$ (for Ln = Nd, Pr, La) was suspended in 20 mL of toluene. To this suspension, 0.5 mmol of EMe_3 was added at ambient temperature and the reaction mixture was allowed to stir for 24 h. After filtration, the solution was concentrated to half of its volume and the complexes were crystallised by layering pentane onto the toluene solution. After 12 h crystals were obtained. The yields of the compounds refer to the amount obtained after a second crystallisation.

[$Cp_2YON(C_2H_4$-*o*-$Py)_2\cdot AlMe_3$] (1): Yield 181 mg (0.34 mmol, 68%). ^{1}H NMR (400 MHz, [D_8]THF, 25 °C): δ = 8.53 (d, 2 H, Ar-C*H*), 7.77 (br. t, 2 H, Ar-C*H*), 7.29 (s, 4 H, 2 Ar-C*H*), 6.13 (s, 10 H, Cp-C*H*), 3.55–3.25 (m, 4 H, 2 CH_2), 3.10–2.75 (m, 4 H, 2 CH_2), –0.88 (s, 9 H, CH_3) ppm. ^{13}C{^{1}H} NMR (100 MHz, [D_8]THF, 25 °C): δ = 160.3 (Ar-C_q), 150.4 (Ar-C), 139.0 (Ar-C), 125.4 (Ar-C), 122.7 (Ar-C), 111.3 (Cp-C), 59.3 (CH_2), 35.0 (CH_2), –4.9 (CH_3) ppm. ^{27}Al NMR (104 MHz, [D_8]THF, 25 °C): δ = 171 ($\nu_{1/2}$ = 4000 Hz) ppm. $C_{27}H_{35}AlN_3OY$ (533.48): calcd. C 60.79, H 6.61, N 7.88; found C 59.84, H 6.54, N 7.63.

[$Cp_2YON(C_2H_4$-*o*-$Py)_2\cdot GaMe_3$] (2): Yield 132 mg (0.23 mmol, 46%). ^{1}H NMR (500 MHz, [D_8]THF, 25 °C): δ = 8.53 (d, $^3J_{HH}$ = 4.7 Hz, 2 H, Ar-C*H*), 7.75 (t, $^3J_{HH}$ = 7.3 Hz, 2 H, Ar-C*H*), 7.30 (d, $^3J_{HH}$ = 7.7 Hz, 2 H, Ar-C*H*), 7.26 (t, $^3J_{HH}$ = 6.2 Hz, 2 H, Ar-C*H*), 6.00 (s, 10 H, Cp-C*H*), 3.25–2.8 (m, 8 H, 4 CH_2), –0.47 (s, 9 H, CH_3) ppm. ^{13}C{^{1}H} NMR (125 MHz, [D_8]THF, 25 °C): δ = 161.2 (Ar-C_q), 150.3 (Ar-C), 138.8 (Ar-C), 125.3 (Ar-C), 122.3 (Ar-C), 110.3 (Cp-C), 59.5 (CH_2), 34.4 (CH_2), –3.5 (CH_3) ppm. $C_{27}H_{35}GaN_3OY$ (576.22): calcd. C 56.28, H 6.12, N 7.29; found C 56.02, H 6.18, N 7.49.

[$Cp_2YON(C_2H_4$-*o*-$Py)_2\cdot InMe_3$] (3): Yield 224 mg (0.36 mmol, 72%). ^{1}H NMR (500 MHz, [D_8]THF, 25 °C): δ = 8.52 (d, $^3J_{HH}$ = 4.7 Hz, 2 H, Ar-C*H*), 7.74 (t, $^3J_{HH}$ = 7.7 Hz, 2 H, Ar-C*H*), 7.31 (d, $^3J_{HH}$ = 7.9 Hz, 2 H, Ar-C*H*), 7.25 (t, $^3J_{HH}$ = 5.9 Hz, 2 H, Ar-C*H*), 5.95 (s, 10 H, Cp-C*H*), 3.1–2.8 (m, 8 H, 4 CH_2), –0.49 (s, 9 H, CH_3) ppm. ^{13}C{^{1}H} NMR (125 MHz, [D_8]THF, 25 °C): δ = 161.5 (Ar-C_q), 150.3 (Ar-C), 138.7 (Ar-C), 125.3 (Ar-C), 122.2 (Ar-C), 110.2 (Cp-C), 59.8 (CH_2), 34.2 (CH_2), –6.2 (CH_3) ppm. $C_{27}H_{35}InN_3OY$ (621.32): calcd. C 52.19, H 5.68, N 6.76; found C 52.36, H 5.47, N 6.79.

[$Cp_2SmON(C_2H_4$-*o*-$Py)_2\cdot AlMe_3$] (4): Yield 72 mg (0.12 mmol, 24%). $C_{27}H_{35}AlN_3OSm$ (594.94): calcd. C 54.51, H 5.93, N 7.06; found C 54.20, H 5.20, N 7.09.

[Cp$_2$SmON(C$_2$H$_4$-*o*-Py)$_2$·GaMe$_3$] (5): Yield 223 mg (0.35 mmol, 70%). ^{1}H NMR (400 MHz, [D$_8$]THF, 25 °C): δ = 9.69 (s, 10 H, Cp-C*H*), 6.80 (br. d, 2 H, Ar-C*H*), 6.32–6.23 (m, 6 H, Ar-C*H*), 5.48 (br. s, 2 H, C*H*$_2$), 5.24 (br. s, 2 H, C*H*$_2$), 3.68 (br. s, 2 H, C*H*$_2$), 1.71 (br. s, 2 H, C*H*$_2$) –0.3 (s, 9 H, C*H*$_3$) ppm. ^{13}C{^{1}H} NMR (100 MHz, [D$_8$]THF, 25 °C): δ = 158.7 (Ar-C$_q$), 151.0 (Ar-C), 138.3 (Ar-C), 121.1 (Ar-C), 119.5 (Ar-C), 103.5 (Cp-C), 65.4 (CH$_2$), 35.3 (CH$_2$), –3.4 (CH$_3$) ppm.

Table 2. Crystal and refinement data for compounds **1**–**17**.

	1	**2**	**3**	**4**	**5**	**6**
Formula	$C_{27}H_{35}N_3OYAl$	$C_{27}H_{35}N_3OYGa$	$C_{27}H_{35}N_3OYIn$	$C_{27}H_{35}N_3OSmAl$	$C_{27}H_{35}N_3OSmGa$	$C_{27}H_{35}N_3ONdIn$
M_r [g mol^{-1}]	533.47	576.21	621.31	594.91	637.65	676.64
Colour	colourless	colourless	colourless	yellow	yellow	blue
T [K]	163(2)	100(2)	100(2)	153(2)	153(2)	100(2)
Crystal size [mm]	0.30 × 0.25 × 0.20	0.30 × 0.25 × 0.22	0.30 × 0.07 × 0.03	0.29 × 0.11 × 0.04	0.29 × 0.17 × 0.05	0.20 × 0.18 × 0.09
Crystal system	orthorhombic	orthorhombic	orthorhombic	orthorhombic	orthorhombic	monoclinic
Space group	$P2_12_12_1$	$P2_12_12_1$	$P2_12_12_1$	$P2_12_12_1$	$P2_12_12_1$	$P2_1/n$
a [Å]	8.780(2)	8.747(1)	8.792(1)	8.853(1)	8.826(2)	9.789(1)
b [Å]	15.162(1)	15.193(2)	15.239(1)	15.266(2)	15.298(2)	16.545(1)
c [Å]	19.780(2)	19.766(1)	20.017(1)	19.834(2)	19.861(3)	16.617(1)
β [°]	–	–	–	–	–	91.48(1)
V [Å^3]	2633.0(5)	2626.8(1)	2681.8 (2)	2680.5(1)	2681.8(6)	2690.4(3)
Z	4	4	4	4	4	4
$\rho_{calcd.}$ [g cm^{-3}]	1.346	1.457	1.539	1.474	1.579	1.671
μ [mm^{-1}]	2.272	3.247	3.036	2.246	3.195	2.788
F(000)	1112	1184	1256	1204	1276	1340
Θ range [°]	4.5 to 27.0	3.1 to 27.5	3.1 to 27.5	1.7 to 31.9	1.7 to 30.0	3.2 to 30.0
Reflns. collected	41233	29033	26507	33081	30961	65475
Unique reflns.	5617	5923	5995	8697	7812	7836
Observed reflns. (2σ)	4849	5595	5334	8388	7276	6574
R_{int}	0.1354	0.0650	0.0760	0.0221	0.0444	0.0410
Data/restrains/param.	5617/0/301	5923/0/301	5995/0/301	8697/0/301	7812/0/301	7836/0/301
GoF (F^2)	1.110	1.040	1.023	1.013	1.033	1.048
R_1, wR_2 [$I > 2\sigma(I)$]	0.0405, 0.0754	0.0249, 0.0561	0.0310, 0.0559	0.0172, 0.0376	0.0321, 0.0662	0.0226, 0.0351
R_1, wR_2 (all data)	0.0558, 0.0805	0.0286, 0.0580	0.0404, 0.0591	0.0184, 0.0380	0.0362, 0.0675	0.0359, 0.0381
Largest diff. peak/hole [e Å^{-3}]	0.438/–0.473	0.320/–0.260	0.441/–0.517	0.691/–0.306	1.521/–0.676	0.636/–0.540
Abs. structure param.	–0.027(6)	–0.002(4)	–0.008(5)	0.010(5)	–0.025(12)	–
CCDC number	763825	763826	763827	763828	763829	763830
	7	**8**	**9**	**10**	**11**	**12**
Formula	$C_{27}H_{35}N_3OPrAl{\cdot}0.5\ C_7H_8$	$C_{27}H_{35}N_3OPrGa{\cdot}0.5\ C_7H_8$	$C_{27}H_{35}N_3OPrIn$	$C_{27}H_{35}N_3OLaAl$	$C_{27}H_{35}N_3OLaGa{\cdot}0.5C_7H_8$	$C_{27}H_{35}N_3OLaIn$
M_r [g mol^{-1}]	631.57	674.28	673.31	583.47	672.28	671.31
Colour	green	green	green	colourless	colourless	colourless
T [K]	100(2)	100(2)	100(2)	153(2)	200(2)	100(2)
Crystal size [mm]	0.24 × 0.12 × 0.05	0.18 × 0.12 × 0.06	0.28 × 0.27 × 0.16	0.20 × 0.14 × 0.08	0.28 × 0.04 × 0.04	0.30 × 0.26 × 0.20
Crystal system	monoclinic	monoclinic	monoclinic	triclinic	monoclinic	monoclinic
Space group	$P2_1/c$	$P2_1/c$	$P2_1/n$	$P\bar{1}$	$P2_1/c$	$P2_1/n$
a [Å]	8.986(1)	9.010(1)	9.779(1)	8.291(1)	8.487(4)	9.806(2)
b [Å]	36.391(1)	36.477(1)	16.528(1)	19.023(1)	36.223(18)	16.614(2)
c [Å]	9.322(1)	9.323(1)	16.617(1)	19.350(1)	10.043(1)	16.639(3)
α [°]	–	–	–	116.13(1)	–	–
β [°]	108.19(1)	108.21(1)	91.39(1)	94.97(1)	105.69(4)	91.49(1)
γ [°]	–	–	–	99.41(1)	–	–
V [Å^3]	2896.0(1)	2910.5(1)	2684.8(1)	2659.5(2)	2973 (2)	2709.9(8)
Z	4	4	4	4	4	4
$\rho_{calcd.}$ [g cm^{-3}]	1.448	1.539	1.666	1.457	1.502	1.645
μ [mm^{-1}]	1.740	2.607	2.675	1.662	2.350	2.429
F(000)	1292	1364	1336	1184	1356	1328
Θ range [°]	2.9 to 30.0	3.0 to 30.0	3.2 to 30.0	1.2 to 30.0	2.6 to 27.5	2.7 to 30.0
Reflns. collected	45896	54463	56369	31183	52539	62284
Unique reflns.	8430	8488	7807	15409	6813	7906
Observed reflns. (2σ)	6657	6933	6735	12797	5237	6902
R_{int}	0.0550	0.0590	0.0500	0.0183	0.0709	0.0387
Data/restrains/param.	8430/1/335	8488/1/335	7807/0/301	15409/0/601	6813/1/335	7906/0/301
GoF (F^2)	1.037	1.030	1.043	1.015	1.046	1.084
R_1, wR_2 [$I > 2\sigma(I)$]	0.0283, 0.0609	0.0340, 0.0749	0.0236, 0.0503	0.0257, 0.0553	0.0364, 0.0685	0.0193, 0.0399
R_1, wR_2 (all data)	0.0444, 0.0654	0.0470, 0.0792	0.0312, 0.0525	0.0362, 0.0590	0.0579, 0.0755	0.0274, 0.0429
Largest diff. peak/hole [e Å^{-3}]	0.960/–1.161	1.551/–1.344	0.814/–0.892	1.045/–0.816	0.849/–1.109	0.677/–0.447
Abs. structure param.	–	–	–	–	–	–
CCDC number	763831	763832	763833	763834	763835	763836

Table 2. *(Continued)*

	13	14	15	16	17
Formula	$C_{30}H_{44}N_3OYAl_2$	$C_{30}H_{44}N_3OYGa_2$	$C_{30}H_{44}N_3OYIn_2$	$C_{30}H_{44}N_3OSmAl_2$	$C_{30}H_{44}N_3OYAlGa$
M_r [g mol^{-1}]	605.55	691.03	781.23	666.99	648.29
Colour	colourless	colourless	colourless	yellow	colourless
T [K]	153(2)	100(2)	100(2)	153(2)	100(2)
Crystal size [mm]	0.12 × 0.08 × 0.04	0.28 × 0.22 × 0.17	0.30 × 0.10 × 0.03	0.34 × 0.21 × 0.08	0.30 × 0.24 × 0.18
Crystal system	orthorhombic	orthorhombic	orthorhombic	orthorhombic	orthorhombic
Space group	$Pna2_1$	$Pna2_1$	$Pca2_1$	$Pna2_1$	$Pna2_1$
a [Å]	17.108(2)	17.037(2)	14.105(1)	17.040(2)	17.050(1)
b [Å]	13.242(2)	13.221(1)	28.829(4)	13.297(2)	13.228(2)
c [Å]	28.946(4)	28.956(1)	16.102(3)	29.149(4)	28.943(2)
β [°]	–	–	–	–	–
V [Å^3]	6557.3(15)	6522.3(1)	6547.6(15)	6604.6(16)	6527.6(9)
Z	8	8	8	8	8
$\rho_{calcd.}$ [g cm^{-3}]	1.227	1.407	1.585	1.342	1.319
μ [mm^{-1}]	1.857	3.430	3.180	1.856	2.646
F(000)	2544	2832	3120	2728	2688
Θ range [°]	1.4 to 27.5	2.9 to 27.5	2.0 to 25.0	1.4 to 30.0	3.2 to 27.5
Reflns. collected	61537	74440	57085	73555	72615
Unique reflns.	15006	14374	11392	18991	14753
Observed reflns. (2σ)	10678	11993	9080	15862	10813
R_{int}	0.0813	0.0690	0.0790	0.0428	0.0628
Data/restrains/param.	15006/1/680	14374/1/680	11392/1/679	18991/1/692	14753/1/658
GoF (F^2)	1.014	1.028	1.038	1.005	1.057
R_1, wR_2 [$I > 2\sigma(I)$]	0.0770, 0.1750	0.0375, 0.0811	0.0432, 0.0637	0.0387, 0.0810	0.0485, 0.0814
R_1, wR_2 (all data)	0.1108, 0.1989	0.0530, 0.0877	0.0682, 0.0699	0.0507, 0.0858	0.0858, 0.0917
Largest diff. peak/hole [e Å^{-3}]	4.401/–0.550	0.398/–0.653	0.856/–0.654	1.755/–0.571	0.718/–0.541
Abs. structure param.	0.367(7)[a]	0.543(5)[a]	0.028(6)	0.262(7)[a]	0.191(5)[a]
CCDC number	763837	763838	763839	763840	763841

[a] Refined as merohedral twins.

[Cp$_2$NdON(C$_2$H$_4$-*o*-Py)$_2$·InMe$_3$] (6): Yield 68 mg (0.10 mmol, 20%).

[Cp$_2$PrON(C$_2$H$_4$-*o*-Py)$_2$·AlMe$_3$] (7): Yield 257 mg (0.44 mmol, 88%). $C_{27}H_{35}AlN_3OPr{\cdot}0.5C_7H_8$ (631.56): calcd. C 57.73, H 6.67, N 6.62; found C 57.18, H 6.51, N 6.60.

[Cp$_2$PrON(C$_2$H$_4$-*o*-Py)$_2$·GaMe$_3$] (8): Yield 107 mg (0.17 mmol, 33%). $C_{27}H_{35}GaN_3OPr{\cdot}0.5C_7H_8$ (674.29): calcd. C 54.09, H 6.25, N 6.20; found C 54.17, H 6.08, N 6.17.

[Cp$_2$PrON(C$_2$H$_4$-*o*-Py)$_2$·InMe$_3$] (9): Yield 283 mg (0.42 mmol, 84%). $C_{27}H_{35}InN_3OPr$ (673.32): calcd. C 48.16, H 5.24, N 6.24; found C 48.36, H 5.16, N 6.20.

[Cp$_2$LaON(C$_2$H$_4$-*o*-Py)$_2$·AlMe$_3$] (10): Yield 64 mg (0.11 mmol, 22%). $C_{27}H_{35}AlLaN_3O$ (583.48): calcd. C 52.19, H 5.68, N 6.76; found C 52.36, H 5.47, N 6.79.

[Cp$_2$LaON(C$_2$H$_4$-*o*-Py)$_2$·GaMe$_3$] (11): Yield 169 mg (0.27 mmol, 54%). ^{1}H NMR (500 MHz, [D$_8$]THF, 25 °C): δ = 8.77 (br. d, 2 H, Ar-C*H*), 7.76 (t, 2 H, Ar-C*H*), 7.30 (m, 4 H, Ar-C*H*), 5.97 (s, 10 H, Cp-C*H*), 3.4–2.8 (m, 8 H, CH_2), –0.56 (s, 9 H, CH_3) ppm. ^{13}C{^{1}H} NMR (125 MHz, [D$_8$]THF, 25 °C): δ = 162.0 (Ar-C$_q$), 150.7 (Ar-C), 138.5 (Ar-C), 125.6 (Ar-C), 122.2 (Ar-C), 111.8 (Cp-C), 60.2 (CH$_2$), 35.0 (CH$_2$), –3.3 (CH$_3$) ppm. $C_{27}H_{35}GaLaN_3O$ (626.22): calcd. C 51.79, H 5.63, N 6.71; found C 51.02, H 5.32, N 6.79.

[Cp$_2$LaON(C$_2$H$_4$-*o*-Py)$_2$·InMe$_3$] (12): Yield 168 mg (0.25 mmol, 50%). ^{1}H NMR (500 MHz, [D$_8$]THF, 25 °C): δ = 8.71 (br. d, 2 H, Ar-C*H*), 7.72 (br. t, 2 H, Ar-C*H*), 7.27 (m, 4 H, Ar-C*H*), 5.95 (s, 10 H, Cp-C*H*), 3.3–2.8 (m, 8 H, CH_2), –0.53 (s, 9 H, CH_3) ppm. ^{13}C{^{1}H} NMR (125 MHz, [D$_8$]THF, 25 °C): δ = 161.8 (Ar-C$_q$), 150.3 (Ar-C), 138.1 (Ar-C), 125.0 (Ar-C), 122.0 (Ar-C), 111.8 (Cp-C), 60.7 (CH$_2$), 34.9 (CH$_2$), –6.1 (CH$_3$) ppm. $C_{27}H_{35}InLaN_3O$ (671.32): calcd. C 48.31, H 5.26, N 6.26; found C 48.76, H 5.40, N 6.08.

General Procedure for the Syntheses of Di-Earth-Metal Alkyl Adducts [Cp$_2$LnON(C$_2$H$_4$-*o*-Py)$_2$·2EMe$_3$] (13–16): Recrystallised [Cp$_2$LnON(C$_2$H$_4$-*o*-Py)$_2$] (0.5 mmol) was suspended in 20 mL of toluene. To this suspension four equivalents of EMe$_3$ (1 mmol) were added at ambient temperature where after the reaction mixture cleared directly. After stirring for 24 h the solution was filtered, concentrated to one fifth of its volume in vacuo and the complexes were crystallised by layering pentane onto the toluene solution. After 12 h crystals were obtained. The yields of the compounds refer to the amount obtained after a second crystallisation.

[Cp$_2$YON(C$_2$H$_4$-*o*-Py)$_2$·2 AlMe$_3$] (13): Yield 115 mg (0.19 mmol, 38%).

[Cp$_2$YON(C$_2$H$_4$-*o*-Py)$_2$·2 GaMe$_3$] (14): Yield 152 mg (0.22 mmol, 44%). ^{1}H NMR (500 MHz, [D$_8$]THF, 25 °C): δ = 8.53 (d, $^3J_{HH}$ = 4.6 Hz, 2 H, Ar-C*H*), 7.76 (t, $^3J_{HH}$ = 7.5 Hz, 2 H, Ar-C*H*), 7.31 (d, $^3J_{HH}$ = 7.8 Hz, 2 H, Ar-C*H*), 7.26 (t, $^3J_{HH}$ = 6.3 Hz, 2 H, Ar-C*H*), 6.00 (s, 10 H, Cp-C*H*), 3.25–2.8 (m, 8 H, CH_2), –0.48 (s, 18 H, CH_3) ppm. ^{13}C{^{1}H} NMR (125 MHz, [D$_8$]THF, 25 °C): δ = 161.1 (Ar-C$_q$), 150.5 (Ar-C), 138.6 (Ar-C), 125.3 (Ar-C), 122.2 (Ar-C), 110.6 (Cp-C), 59.5 (CH$_2$), 34.5 (CH$_2$), –4.1 (CH$_3$) ppm. $C_{30}H_{44}Ga_2N_3OY$ (691.04): calcd. C 52.14, H 6.42, N 6.08; found C 52.57, H 6.65, N 5.98.

[Cp$_2$YON(C$_2$H$_4$-*o*-Py)$_2$·2 InMe$_3$] (15): Yield 136 mg (0.17 mmol, 35%). ^{1}H NMR (500 MHz, [D$_8$]THF, 25 °C): δ = 8.54 (d, $^3J_{HH}$ = 4.6 Hz, 2 H, Ar-C*H*), 7.77 (t, $^3J_{HH}$ = 7.7 Hz, 2 H, Ar-C*H*), 7.35 (d, $^3J_{HH}$ = 7.8 Hz, 2 H, Ar-C*H*), 7.28 (t, $^3J_{HH}$ = 6.3 Hz, 2 H, Ar-C*H*), 6.01 (s, 10 H, Cp-C*H*), 3.25–2.8 (m, 8 H, CH_2), –0.45 (s, 18 H, CH_3) ppm. ^{13}C{^{1}H} NMR (125 MHz, [D$_8$]THF, 25 °C): δ = 161.6 (Ar-C$_q$), 150.6 (Ar-C), 139.0 (Ar-C), 125.5 (Ar-C), 122.6 (Ar-C),

110.5 (Cp-C), 60.0 (CH_2), 34.6 (CH_2), –6.1 (CH_3), ppm. $C_{30}H_{44}In_2N_3OY$ (781.24): calcd. C 46.12, H 5.68, N 5.38; found C 46.04, H 5.71, N 5.22.

[Cp$_2$SmON(C$_2$H$_4$-*o*-Py)$_2$·2 AlMe$_3$] (16): Yield 240 mg (0.36 mmol, 72%). ^{1}H NMR (400 MHz, [D$_8$]THF, 25 °C): δ = 10.02 (s, 10 H, Cp-C*H*), 7.05 (s, 2 H, Ar-C*H*), 6.70 (s, 2 H, Ar-C*H*), 6.23 (s, 2 H, Ar-C*H*), 5.50 (s, 2 H, CH_2) 5.16 (br. s, 2 H, Ar-C*H*), 5.00 (s, 2 H, CH_2), 4.20 (s, 2 H, CH_2), 2.55 (s, 2 H, CH_2) –1.00 (s, 18 H, CH_3) ppm. ^{13}C{^{1}H} NMR (100 MHz, [D$_8$]THF, 25 °C): δ = 158.9 (Ar-C$_q$), 150.8 (Ar-C), 138.9 (Ar-C), 122.1 (Ar-C), 120.2 (Ar-C), 105.8 (Cp-C), 65.4 (CH_2), 36.8 (CH_2), –7.2 (CH_3) ppm. ^{27}Al NMR (104 MHz, [D$_8$]THF, 25 °C): δ = 180 ($\nu_{1/2}$ = 3000 Hz) ppm. $C_{30}H_{44}Al_2N_3OSm$ (667.02): calcd. C 54.02, H 6.65, N 6.30; found C 53.46, H 6.35, N 6.40.

[Cp$_2$YON(C$_2$H$_4$-*o*-Py)$_2$·AlMe$_3$·GaMe$_3$] (17): Recrystallised **1** (267 mg, 0.5 mmol) was suspended in 20 mL of toluene. To this suspension 1.1 equiv. of GaMe$_3$ (63 mg, 0.55 mmol) were added at ambient temperature and the reaction mixture cleared directly. After stirring for 24 h the solution was filtered, concentrated to one tenth of its volume in vacuo and the complex was crystallised by layering pentane onto the toluene solution. After 12 h crystals were obtained. The yields of the compound refer to the amount obtained after first crystallisation. Yield 104 mg (0.16 mmol, 32%). ^{1}H NMR (600 MHz, [D$_8$]THF, 25 °C): δ = 8.54 (br. d, 2 H, Ar-C*H*), 7.78 (br. t, 2 H, Ar-C*H*), 7.30 (s, 4 H, Ar-C*H*), 6.12 (s, 10 H, Cp-C*H*), 3.55–3.25 (m, 4 H, CH_2), 3.10–2.75 (m, 4 H, CH_2), –0.49 (s, 9 H, Ga-CH_3), –0.88 (s, 9 H, Al-CH_3) ppm. ^{13}C{^{1}H} NMR (100 MHz, [D$_8$]THF, 25 °C): δ = 160.4 (Ar-C$_q$), 150.4 (Ar-C), 139.0 (Ar-C), 125.4 (Ar-C), 122.8 (Ar-C), 111.3 (Cp-C), 59.2 (CH_2), 35.0 (CH_2), –4.5 (Al-CH_3), –5.2 (Ga CH_3) ppm. ^{27}Al NMR (104 MHz, [D$_8$]THF, 25 °C): δ = 171 ($\nu_{1/2}$ = 3500 Hz) ppm. $C_{30}H_{44}AlGaN_3OY$ (648.31): calcd. C 60.79, H 6.61, N 7.88; found C 59.84, H 6.54, N 7.63.

Supporting Information (see footnote on the first page of this article): Figure S1 contains ^{1}H and ^{13}C NMR spectra of complex **2**, Figure S2 its HMQC-NMR spectrum, Figure S3 VT-NMR spectra and Figure S4 its ^{1}H-^{1}H-COSY-NMR spectrum. Figure S5 contains a ^{13}C-NMR spectrum of **11**, Figure S6 the HMBC-NMR spectrum of **14**; Figure S8 a section of the ^{1}H-NMR of **14** at –50 °C, Figure S9 the ^{1}H-NMR and Figure S10 the ^{13}C-NMR spectrum of **15**; Figure S11 shows ^{1}H-NMR spectra at 50 °C, Figure S12 the HMBC-NMR spectrum at –80 °C and Figure S13 the HMQC-NMR spectrum at –70 °C of **17**.

Acknowledgments

We thank Dr. A. Hepp (University of Münster, Germany) for measuring parts of the NMR spectra, G. Schön for CHN analyses and T. Pape for parts of the X-ray data collection, as well as the project students A. Stute (Münster) and L. Schachtsiek (Bielefeld) for their help in laboratory. We are grateful to the Fonds der Chemischen Industrie for the financial support.

[1] a) A. P. Dove, X. Xie, R. M. Waymouth, *Chem. Commun.* **2005**, 2152; b) R. Wang, X. Zhang, S. Chen, X. Yu, C. Wang, D. B. Beach, Y. Wu, Z. Xue, *J. Am. Chem. Soc.* **2005**, *127*, 5204; c) N. W. Mitzel, S. Parsons, A. J. Blake, D. W. H. Rankin, *J. Chem. Soc., Dalton Trans.* **1996**, 2098; d) K. Wieghardt, I. Tolksdorf, J. Weiss, W. Swiridoff, *Z. Anorg. Allg. Chem.* **1982**, *490*, 182; e) A. Willner, J. Niemeyer, N. W. Mitzel, *Dalton Trans.* **2009**, 4473.

[2] a) S. Jana, R. J. F. Berger, R. Fröhlich, N. W. Mitzel, *Chem. Commun.* **2006**, 3993; b) M. Ullrich, R. J. F. Berger, C. Lustig, R. Fröhlich, N. W. Mitzel, *Eur. J. Inorg. Chem.* **2004**, 397.

[3] a) P. Bösing, A. Willner, T. Pape, A. Hepp, N. W. Mitzel, *Dalton Trans.* **2008**, 2549; b) N. W. Mitzel, C. Lustig, M. Woski, *Dalton Trans.* **2004**, 397; c) C. Lustig, N. W. Mitzel, *Angew. Chem.* **2001**, *113*, 4521; C. Lustig, N. W. Mitzel, *Angew. Chem. Int. Ed.* **2001**, *40*, 4390.

[4] a) N. W. Mitzel, A. J. Blake, D. W. H. Rankin, *J. Am. Chem. Soc.* **1997**, *119*, 4143; b) N. W. Mitzel, U. Losehand, *Angew. Chem.* **1997**, *109*, 2897; *Angew. Chem. Int. Ed. Engl.* **1997**, *36*, 2807; c) N. W. Mitzel, U. Losehand, *J. Am. Chem. Soc.* **1998**, *120*, 7320; d) U. Losehand, N. W. Mitzel, *Inorg. Chem.* **1998**, *37*, 3175; e) N. W. Mitzel, U. Losehand, A. Wu, D. Cremer, D. W. H. Rankin, *J. Am. Chem. Soc.* **2000**, *112*, 4471; f) N. W. Mitzel, K. Vojinović, R. Fröhlich, T. Foerster, D. W. H. Rankin, *J. Am. Chem. Soc.* **2005**, *127*, 1370; g) M. Woski, R. J. F. Berger, N. W. Mitzel, *Dalton Trans.* **2008**, 5652.

[5] a) N. W. Mitzel, K. Vojinović, *J. Chem. Soc., Dalton Trans.* **2002**, 2341; b) N. W. Mitzel, U. Losehand, S. L. Hinchley, D. W. H. Rankin, *Inorg. Chem.* **2001**, *40*, 661.

[6] a) S. Jana, R. Fröhlich, R. J. F. Berger, N. W. Mitzel, *Chem. Commun.* **2006**, 3993; b) M. Ullrich, C. Lustig, R. J. F. Berger, R. Fröhlich, N. W. Mitzel, *Eur. J. Inorg. Chem.* **2006**, 4219.

[7] S. Jana, T. Pape, N. W. Mitzel, D. W. H. Rankin, *Z. Naturforsch., Teil B* **2007**, *62*, 1339.

[8] A. S. R. Chesman, D. R. Turner, E. I. Izgorodina, S. R. Batten, G. B. Deacon, *Dalton Trans.* **2007**, 1371.

[9] A. Venugopal, A. Hepp, T. Pape, A. Mix, N. W. Mitzel, *Dalton Trans.* **2008**, 6628.

[10] A. Venugopal, R. J. F. Berger, A. Willner, T. Pape, N. W. Mitzel, *Inorg. Chem.* **2008**, *47*, 4506.

[11] A. Venugopal, A. Willner, A. Hepp, N. W. Mitzel, *Dalton Trans.* **2007**, 3124.

[12] A. Venugopal, A. Willner, K. Bergander, A. Hepp, N. W. Mitzel, *Dalton Trans.* **2009**, 5715.

[13] W. J. Evans, J. M. Perotti, R. J. Doedens, J. W. Ziller, *Chem. Commun.* **2001**, 2326.

[14] B. J. Hellmann, A. Venugopal, A. Mix, B. Neumann, H.-G. Stammler, A. Willner, T. Pape, A. Hepp, N. W. Mitzel, *Chem. Eur. J.* **2009**, *15*, 11701.

[15] C. Lustig, Dissertation, Technische Universität München, **2002**.

[16] J. L. Atwood, R. D. Priester, R. D. Rogers, L. G. Canada, *J. Inclusion Phenom. Mol. Recognit. Chem.* **1983**, *1*, 61.

[17] J. L. Atwood, G. D. Stucky, *J. Am. Chem. Soc.* **1967**, *89*, 5362.

[18] W. J. Evans, T. J. Boyle, J. W. Ziller, *J. Am. Chem. Soc.* **1993**, *115*, 5084.

[19] A. A. R. Sayigh, H. Ulrich, M. Green, *J. Org. Chem.* **1964**, *29*, 2042.

[20] N. W. Mitzel, B. A. Smart, S. Parsons, H. E. Robertson, D. W. H. Rankin, *J. Chem. Soc. Perkin Trans. 2* **1996**, 2727.

[21] G. H. Robinson, W. E. Hunter, S. G. Bott, J. L. Atwood, *J. Organomet. Chem.* **1987**, *326*, 9.

[22] C. W. Belock, A. Çetin, N. V. Barone, C. J. Ziegler, *Inorg. Chem.* **2008**, *47*, 7114.

[23] W. Wang, Y. Pan, X. Huang, H. Sun, Z. Lu, X. Sun, *Acta Crystallogr., Sect. C: Cryst. Struct. Commun.* **1996**, *52*, 1661.

[24] G. Rossetto, N. Brianese, A. Camporese, U. Casellato, F. Ossola, M. Porchia, P. Zanella, R. Graziani, *Gazz. Chim. Ital.* **1990**, *120*, 805.

[25] H. Schumann, T. D. Seuß, O. Just, R. Weimann, H. Hemling, F. H. Görlitz, *J. Organomet. Chem.* **1994**, *479*, 171.

[26] H.-S. Sun, X.-M. Wang, X.-Z. You, X.-Y. Huang, *Polyhedron* **1995**, *14*, 2159.

[27] F. Thomas, T. Bauer, S. Schulz, M. Nieger, *Z. Anorg. Allg. Chem.* **2003**, *629*, 2018.

[28] D. Ogrin, L. H. van Poppel, S. G. Bott, A. R. Barron, *Dalton Trans.* **2004**, 3689.

[29] H. Friebolin, *Ein- und zweidimensionale NMR-Spektroskopie*, vol. 1, VCH Verlagsgesellschaft, Weinheim (Germany), **1988**, p. 241.
[30] J. M. Birmingham, G. Wilkinson, *J. Am. Chem. Soc.* **1956**, *78*, 42.
[31] G. M. Sheldrick, *Program for Refinement of Structures*, University of Göttingen, **1997**.
[32] M. N. Burnett, C. K. Johnson, *ORTEP-III: Oak Ridge Thermal Ellipsoid Plot Program for Crystal Structure Illustrations*, Oak Ridge National Laboratory Report ORNL-6895, **1996**.
Received: February 2, 2010
Published Online: May 4, 2010

